Power Generation Efficiency of an SOFC-PEFC Combined System with Time Shift Utilization of SOFC Exhaust Heat

Shin'ya OBARA
Power Engineering Lab., Department of Electrical and Electronic Engineering, Kitami Institute of Technology
165 Kouen-cho, Kitami, HOKKAIDO 0908507, Japan
Phone/Fax +157-26-9262
e-mail: obara@indigo.plala.or.jp

Abstract
A microgrid, with little environmental impact, is developed by introducing a combined SOFC (solid oxide fuel cell) and PEFC (proton exchange membrane fuel cell) system. Although the SOFC requires a higher operation temperature compared to the PEFC, the power generation efficiency of the SOFC is higher. However, if high temperature exhaust heat may be used effectively, a system with higher total power generation efficiency can be built. Therefore, this paper investigates the operation of a SOFC-PEFC combined system, with time shift operation of reformed gas, into a microgrid with 30 houses in Sapporo, Japan. The SOFC is designed to correspond to base load operation, and the exhaust heat of the SOFC is used for production of reformed gas. This reformed gas is used for the production of electricity for the PEFC, corresponding to fluctuation load of the next day. Accordingly, the reformed gas is used with a time shift operation. In this paper, the relation between operation method, power generation efficiency, and amount of heat storage of the SOFC-PEFC combined system to the difference in power load pattern was investigated. The average power generation efficiency of the system can be maintained at nearly 48% on a representative day in February (winter season) and August (summer season).

Keywords (5-10): Fuel Cell, Micro-Grid, Combined System, SOFC, PEFC, Operation Planning.

1. Introduction

PEFC (proton exchange membrane fuel cell) and SOFC (solid oxide type fuel cell) have been developed as fuel cells for houses [1-3]. The SOFC requires a higher operation temperature compared to the PEFC. However, the power generation efficiency is higher in SOFCs, and high temperature exhaust heat can be widely used. The SOFC-GT (gas turbine) combined system was developed as an effective method to use the high temperature exhaust heat of SOFC [4-8]. In this combined system, the exhaust heat of the SOFC is used as a heat source in the heat transfer medium of the GT. Generally, calculations for the efficiency of an energy system require knowledge about the load pattern. Operation of the GT is dependent on the amount of exhaust heat of the SOFC. Furthermore, the exhaust heat of the SOFC and operation of the GT synchronize. Therefore, the load following operation of a microgrid using the SOFC-GT combined system cannot maintain high thermal efficiency. In the combined system with the load following operation of the GT, and base load operation of the SOFC, since the partial-load characteristic of the GT is poor, the power generation efficiency of the whole system is not high. In the combined system with the base load operation of the GT and load following operation of the SOFC, since the exhaust heat of the SOFC is not stabilized, the production of electricity of the GT is restricted. Moreover, the power generation efficiency during partial-load of the SOFC is greatly reduced compared to full-load operation. Consequently, in order to obtain high power generation efficiency with the SOFC-GT

combined system, either storage-of-electricity equipment needs to be installed or uniform system load is required. Therefore, this paper examines a system which produces reformed gas with high hydrogen concentration using the exhaust heat of the SOFC. The system is characterized by the ability to shift the utilization time of the produced reformed gas. Flexible operation can be planned because it is not necessary to synchronize the exhaust heat output of the SOFC and utilization of the reformed gas. In this paper, the installation of a SOFC-PEFC combined system into a microgrid used for supplying energy to 30 houses in Sapporo, Japan is assumed. The SOFC is made to correspond to the base load operation of the microgrid, and the PEFC is made to correspond to the fluctuation load in the proposal system. In this case, reformed gas is produced by supplying the exhaust heat of the SOFC to a steam reformer using natural gas. This reformed gas is stored, and the system operation method for the next day is planned with reference to the amount of stored reformed gas. In this study, fuel consumption of all equipment, power generation efficiency, and operation method of heat storage and boiler, when operating the SOFC-PEFC combined system under different load patterns, is investigated. From this result, the load characteristics of the system and average power generation efficiency when installing the proposed system into the microgrid are elucidated.

2. System Scheme

2.1 Microgrid model

Figure 1 shows a power system model of a microgrid with 30 houses. This microgrid is installed into a residential area; power and heat are supplied by introducing a SOFC-PEFC combined system. The SOFC outputs high temperature exhaust heat at 750 to 900 degrees Celsius. In this study, a steam reformer of natural gas is operated using this high temperature exhaust heat. The reformed gas is stored in a cylinder, and the stored gas can be supplied to the PEFC at an arbitrary time. Flexible operation can be planned because the exhaust heat of the SOFC and power generation of the PEFC is not synchronized. On the other hand, load with various fluctuations added to the microgrid is expected. Accordingly, this study investigates operation of the SOFC-PEFC combined system using three different power load patterns.

2.2 SOFC-PEFC combined system

(1) Power system

Figure 2 is the block diagram of the SOFC-PEFC combined system examined in this paper. The SOFC installed into the system assumes an internal reforming type. Natural gas and air for supplying the SOFC are heated by the SOFC exhaust through a heat exchanger (HEX). The exhaust heat of the SOFC is supplied to a steam reformer (R/M) of natural gas, and reformed gas with high hydrogen concentration is produced. Water contained in the reformed gas is removed with an air-cooling condenser (C/S). After reducing the carbon monoxide in the reformed gas to several ppm by using CO oxidation equipment (C/O), the reformed gas is stored in a cylinder. The reformed gas stored in the cylinder can be supplied to the PEFC at a later time. The power of the SOFC and PEFC is supplied to DC-DC and DC-AC converters. Finally, after changing this power to the target voltage and frequency through an inverter, the power is supplied to the microgrid.

(2) Heat system

First, the exhaust heat of the SOFC is used for heating natural gas and air. The remaining exhaust heat is supplied to the steam reformer (R/M) of natural gas. The exhaust heat of the natural gas steam reformer is stored in a heat storage tank.

A heat exchanger is installed in the heat storage tank, and heat is exchanged between tap water and heat medium. A boiler is operated when the temperature of the heated tap water does not meet demand.

2.3 Operation method of the system

Figure 3 shows the power operation model of the SOFC-PEFC combined system introduced into the microgrid.

(1) Model A

In Model A, shown in Fig. 3 (a), Fuel cell A corresponds to base load operation of the microgrid, and Fuel cell B corresponds to fluctuation load. Here, the base load of Model A is set up smaller than the minimum of the load fluctuation. In this case, Fuel cell A is operated at maximum power generation efficiency at all times.

(2) Model B

In Model B shown in Fig. 3 (b), in order to make the power of Fuel cell A increase, the base load by Fuel cell A is set as the minimum of load fluctuation. Describe in the next Section, the maximum power generation efficiency of SOFC is high compared with PEFC. So, the SOFC is introduced into Fuel cell A in each model in Fig. 3. Because the amount of exhaust heat by the SOFC-PEFC combined system changes with the operating method of the SOFC, the amount of production of reformed gas changes by load setup of Fuel cell A.

(3) Model C

In this paper, the reforming gas consumed on the next day is manufactured using the exhaust heat of the SOFC by Fuel cell B (that is, the PEFC). In this case, the operation method of Model C, shown in Fig. 3 (c), can be considered. In Model C, the load of Fuel cell A increases compared with Model B. When a part of the base load area is included to the fluctuating load area, Fuel cell A is accompanied by partial-load operation.

The characteristics of each model of Fig. 3 are highly efficient SOFC under the base load and PEFC with good efficiency under the partial load corresponds to the fluctuation load. As a result, the power generation efficiency of the system increases. Furthermore, since the reforming gas produced by the exhaust heat of the SOFC can be used at a later time, operation of the system becomes flexible. Because the load of the SOFC of Model C can be set up most highly, it is expected that system overall efficiency improves greatly.

2.4 Partial-load characteristics of fuel cells

Figure 4 (a) shows the relationship between the load factor of the SOFC and power generation efficiency with internal reforming [9]. Figure 4 (b) is the relationship between the output of the reforming gas and reformer efficiency of steam reforming using natural gas [10]. Furthermore, Fig. 4 (c) shows the relationship between the load factor of the PEFC with the reformer, and power generation efficiency [11-15]. When Fig. 4 (a) is compared with Fig. 4 (c), the SOFC shows greater power generation efficiency compared with the PEFC for 25% or more of the load factor. When operating the SOFC with 25% or less of the load factor, power generation efficiency decreases drastically. Therefore, operation of the SOFC at 25% or less of the load factor is not generally assumed. The power generation efficiency of the SOFC differs by nearly 21% for load factors of 25% and 100%. On the other hand, the power generation efficiency of the PEFC differs by nearly 11% for load factors of 15% and 100%.

The performance of R/M, S/U, and C/O is dependent on the reformer efficiency, shown in Fig. 4 (b). Equation (1) is the definitional equation of reformer efficiency.

$$\eta_R = \frac{\text{Lower heating value of the reformed gas}}{\text{Natural gas supply (heating value)}} \times 100 \quad (1)$$

According to the difference of the output of reformed gas, reformer efficiency differs by less than 10% (Fig. 4 (b)). As for Fuel cell A, shown in Model C in Fig. 3 (c), partial-load operation is included. In this case, because the amount of exhaust heat supplied to the reformer is reduced, the output of reformed gas decreases. However, production of reformed gas is stable relative to reformer efficiency and reformed gas output, shown in Fig. 4 (b).

2.5 Time shift utilization of the reformed gas

This section describes the analysis method of the SOFC-PEFC combined system with time shift utilization of the SOFC exhaust heat. In order to obtain the reformed gas supplied to the PEFC, it is necessary to increase the capacity of the SOFC. On the other hand, to reduce equipment costs, the installed capacity of the SOFC needs to be decreased. Figure 5 (a) shows the pattern of each operating method of the SOFC and PEFC. If the SOFC is made to correspond to the base load operation, shown in Fig. 5 (a), exhaust heat shown in Fig. 5 (b) will be outputted. The steam reformer of natural gas is operated using this exhaust heat, and the reformed gas shown in Fig. 5 (c) is produced. This stored reformed gas is used for the operation of the PEFC for the next day (Fig. 5 (d)).

Here, the capacity of the SOFC and PEFC is set using the following procedure.

a. Randomly set the capacity of the SOFC and PEFC at first. The value of the base load shown in Fig. 5 (a) is the same as the capacity of the SOFC.

b. Obtain the amount of exhaust heat of the SOFC (Fig. 5 (b)) from Fig. 4 (a).

c. The amount of reformed gas produced (Fig. 5 (c)) is calculated from the relationship between the reformer efficiency; output of reformed gas shown in Fig. 4 (b) and amount of exhaust heat expelled by the SOFC (Fig. 5 (b)).

d. Operation of the PEFC for the next day is planned by using the reformed gas described in c. The PEFC is made to correspond to the fluctuation load operation shown in Fig. 5 (a). Therefore, if the load pattern of the next day is the same as the load pattern of a representative day, the capacity of the SOFC and PEFC will satisfy the power demand (base and fluctuating loads), shown in Fig. 5 (a).

e. Calculate the power balance of the system and reformed gas from the operation plan of the next day. When an error is found in each balance, b. is recalculated for different capacities of the SOFC and PEFC.

f. Repeat calculation of b. to e. until the power balance error of the system and reformed gas is less than 0.1%. When the error is less than 0.1%, the capacity of the SOFC and PEFC is considered optimized.

In the analysis of this paper, operation is planned so that the balance of power and heat may be satisfied, and a detailed physical model does not introduce.

3. Analysis Conditions

(1) Load model

In this analysis example, the microgrid is installed into 30 houses in Sapporo, Japan. Figure 6 shows the power and heat demand model in 30 houses in Sapporo [16]. Air conditioning is not used during the summer season (from July to September) in Sapporo. Moreover, the heating load during the winter season (from November to March) is contained in the heat load shown in Fig. 6 (b). Therefore, the electricity demand model, shown in Fig. 6 (a), is mainly the load from lighting and household appliances. In the SOFC-PEFC combined system, the amount of reformed gas produced

changes with the operating methods of the SOFC. For this reason, the power demand pattern of the microgrid has a large influence on operation plan of the system. Accordingly, this paper investigates two patterns based on the power demand pattern shown in Fig. 6 (a). Figures 7 (a) and (b) are compressions of the width of daily load fluctuations (compressed load pattern) and extensions of the width of daily load fluctuations (extended load pattern), respectively. These patterns compress and extend fluctuations of the average load of power demand on a representative day to 50%, and 150%, respectively. Here the load integration value (the amount of power demand on the representative day) of both patterns is the same as the total power demand under average load. As a result, this paper investigates the electricity demand model of the microgrid of three patterns, shown in Fig. 8 (this figure is an example of a representative day in February).

(2) Equipment characteristic

The following equipment characteristics are used in the analysis. The heat storage tank assumes 0.5% per hour of loss; and boiler efficiency is set to 90%. In the analysis, power consumption of the auxiliary machinery used to maintain operation of the system, such as the blower, pump, and controller, is not taken into consideration. Moreover, power consumption of the compressor used for storage of the reformed gas is not taken into consideration because it is small compared with the power demand. Each setting value described in the top is a general actual value.

4. Analysis Result

4.1 Operation plan in a representative day

Figure 9 shows the result of the operation analysis of the independent SOFC , independent PEFC , and SOFC-PEFC combined systems in a representative day in February (winter season) and August (summer season). The analysis results of the relationship between the load factor and power generation efficiency, fuel consumption in the boiler and fuel cell, and heat storage plan of each system are shown in Fig. 9. The maximum power load of the microgrid shown in Fig. 6 (a) appears in February. Therefore, the capacity of the SOFC and PEFC should be optimized under electricity demand mode in a representative day in February. As a result, considering the maximum power load in a representative day in February, the capacity of the SOFC and PEFC was set to 23 kW. The operation analysis in the individual operation of the SOFC and PEFC also uses this capacity (23 kW). On the other hand, the load of the SOFC-PEFC combined system must combine the power load and load from the production of reformed gas. For this reason, the total capacity of the SOFC and PEFC exceeds 23 kW. The capacity of the SOFC and PEFC with an average load pattern (Fig. 8), calculated from the operation analysis described in Section 2.5, is 17.6 kW and 6.8 kW, respectively.

When the SOFC or PEFC is made to correspond to load fluctuation independently (Fig. 9a and Fig. 9b), there is little difference between the fuel consumption of SOFC to PEFC. This reason for the difference is in the load characteristic of each fuel cell, shown in Figs. 4 (a) and (c). On the other hand, the SOFC independent system consumes more boiler fuel in August. This is because the power generation efficiency of the SOFC is high, so there is little exhaust heat expelled. For the same reason, the capacity of the heat storage tank of the SOFC independent system is small compared with that of the PEFC independent system. Figure 9 (c) shows the analysis result of the SOFC-PEFC combined system. The result of the load factor and power generation efficiency of the SOFC and PEFC is shown on the left-hand side for every month. The load factor of the SOFC was almost constant except for 0:00 to 4:00. In other words, partial-load operation was seen from 0:00 to 4:00. Therefore, the operation method of both months in Fig. 9 (c) is that of Model C, shown in Fig. 3 (c). Since reformed gas is produced in the SOFC-PEFC combined system using the exhaust

heat of the SOFC, there is little remaining exhaust heat. As a result, the capacity of the heat storage tank of the SOFC-PEFC combined system is the smallest of all the systems.

4.2 Influence of the load pattern

Figures 10 and 11 show the operation analysis result of the SOFC-PEFC combined system analyzed using the compressed (Fig. 7) and extended (Fig. 8) load patterns. When load patterns differ, the combination of the capacity of SOFC and PEFC differs. The main reason for this is that the maximum load changes with load patterns. As a result of the operation analysis described in Section 2.5, the capacity of the SOFC and PEFC is calculated to be 14.2 kW and 4.9 kW under the compressed load pattern, respectively. On the other hand, each capacity is 21.8 kW and 7.4 kW under the extended load pattern. As shown on the left side of Fig. 10 (a), the load factor of the SOFC in February under the compressed load pattern is almost constant. The load factor of the SOFC in a representative day in August, shown on the left side of Fig. 10 (b), changes slightly between 0:00 and 4:00. On the other hand, as shown on the left of Fig. 11 (a) and (b), there is a large change between 0:00 and 6:00 and a small change between 14:00 and 16:00 in the load factor of the SOFC in a representative day in February and August under the extended load pattern. The difference in the load pattern of the microgrid gives the change in the load factor of the SOFC-PEFC combined system, and influences power generation efficiency. As a result, the fuel consumption of and amount of exhaust heat generated by the system also change. During extended load pattern operation, the capacity of the heat storage tank is small, which results from the difference in the amount of exhaust heat.

4.3 Fuel consumption and power generation efficiency

Figure 12 shows the analysis result of fuel consumption of the independent SOFC, independent PEFC, and SOFC-PEFC combined systems for a representative day every month. The average load pattern was used in this analysis. Total fuel consumption is strongly influenced by heat load every month, with the exception of the summer season, since there is more heat compared to electricity demand. On the other hand, since there is no large monthly difference in power load, the fuel consumption of the fuel cell shows few differences over the course of a year. The independent PEFC system clearly consumes more total fuel as compared with the other systems (Fig. 12 (b)). This is because the average power generation efficiency of the PEFC in the power load pattern is low compared with the independent SOFC and SOFC-PEFC combined systems.

Figure 13 shows the average value of the load factor and power generation efficiency of each system in a representative day for every month. The average load pattern was used in this analysis. In the SOFC-PEFC combined system, the load is added to the SOFC by production of reformed gas. By increasing the load factor in the SOFC and using time shift utilization of the exhaust heat, the power generation efficiency in the proposed system is high compared with the other systems. The average power generation efficiency of the proposed system can be maintained at nearly 48% every month.

4.4 Evaluation of the SOFC-PEFC combined system

Figure 14 shows analysis results of the average power generation efficiency of each system in representative day every month using three load patterns (average, compressed and extended load pattern). If the compressed load pattern is installed into the SOFC-PEFC combined system, the highest average power generation efficiency can be obtained. On the other hand, the independent PEFC load following operation shows the lowest average power generation efficiency.

Figure 15 shows the results of each system when using the analysis results of the annual average of the SOFC independent system under 100% average load. The load factor of the SOFC-PEFC combined system rises nearly 20% compared with other systems. As a result, the power generation efficiency of the system increases nearly 4% compared with the SOFC independent system. Although the fuel consumption in the fuel cell of the SOFC-PEFC combined system is reduced by 11% compared with the SOFC independent system, the boiler fuel consumption of the proposal system increases as a result of the amount of exhaust heat. Therefore, the total fuel consumption of the SOFC-PEFC combined system is only reduced by 1% compared with the independent SOFC system. Figure 16 shows the operation result when installing each load pattern into the SOFC-PEFC combined system. The average load pattern was installed in the analysis of this figure. Moreover, the operation result of the annual average was set to 100%. The load factor of the fuel cell shows nearly 43% of difference by the difference in the load pattern, and power generation efficiency occurs 13% of difference. However, when the fuel consumption of the boiler is taken into consideration, the difference in total fuel consumption is 3%. In this case, since there is a large space heating demand in the microgrid, the fuel consumption reduction of the fuel cell becomes small.

5. Conclusions

In this paper, the operation plan of the SOFC-PEFC combined system with time shift utilization of the SOFC exhaust heat is investigated. The analysis assumed installation of the proposed system into a microgrid which consists of 30 houses in Sapporo, Japan. The relationship between the difference in load pattern, operation method of the SOFC-PEFC combined system, power generation efficiency, and amount of heat storage was examined. As a result, the following conclusions were obtained.

The load factor of the SOFC-PEFC combined system increases compared with other systems. This is a result of reformed gas production using the exhaust heat of the SOFC. The reformed gas is used for the operation of the PEFC on the following day. The average power generation efficiency of the system can be maintained at nearly 48% (efficiency) on a representative day every month. This value is a 6% (percentage changes) improvement over independent SOFC operation. Moreover, compared with the independent PEFC operation, it is a 32% (percentage changes) improvement. However, because the load factor of the fuel cell falls as the width of the daily power load fluctuation increases, the average power generation efficiency falls. When the width of the power load fluctuation in a representative day is ±50% of the average value, the difference in average power generation efficiency of the system is nearly 13% (efficiency). As a result of reformed gas production in the SOFC-PEFC combined system using the SOFC exhaust heat, there is little remaining exhaust heat. As a result, the capacity of the heat storage tank of the proposed combined system is small, and the fuel consumption of the boiler increases. The total fuel consumption of the SOFC-PEFC combined system serves as a slight reduction compared with individual SOFC operation.

Acknowledgments

This work was partially supported by a Grant-in-Aid for Scientific Research(C) from JSPS.KAKENHI (20560204).

References

[1] Naim H. Afgan, Maria G. Carvalho, Sustainability assessment of hydrogen energy systems, International Journal of Hydrogen Energy, Vol. 29, No. 13, (2004), 1327-1342.

[2] Muhsin Tunay Gencoglu, Zehra Ural, Design of a PEM fuel cell system for residential application,

International Journal of Hydrogen Energy, Vol. 34, No. 12, (2009), 5242-5248.

[3] Georg Erdmann, Future economics of the fuel cell housing market, International Journal of Hydrogen Energy, Vol. 28, No. 7, (2003), 685-694.

[4] Tak-Hyoung Lim, Rak-Hyun Song, Dong-Ryul Shin, Jung-Il Yang, Heon Jung, I.C. Vinke, Soo-Seok Yang, Operating characteristics of a 5 kW class anode-supported planar SOFC stack for a fuel cell/gas turbine hybrid system, International Journal of Hydrogen Energy, Vol. 33, No. 3, (2008), 1076-1083.

[5] S. H. Chan, H. K. Ho, Y. Tian, Multi-level modeling of SOFC–gas turbine hybrid system, International Journal of Hydrogen Energy, Vol. 28, No. 8, (2003), 889-900.

[6] Ali Volkan Akkaya, Bahri Sahin, Hasan Huseyin Erdem, An analysis of SOFC/GT CHP system based on exergetic performance criteria, International Journal of Hydrogen Energy, Vol. 33, No. 10, (2008), 2566-2577.

[7] Sadegh Motahar, Ali Akbar Alemrajabi, Exergy based performance analysis of a solid oxide fuel cell and steam injected gas turbine hybrid power system, International Journal of Hydrogen Energy, Vol. 34, No. 5, (2009), 2396-2407.

[8] Y. Haseli, I. Dincer, G.F. Naterer, Thermodynamic modeling of a gas turbine cycle combined with a solid oxide fuel cell, International Journal of Hydrogen Energy, Vol. 33, No. 20, (2008), 5811-5822.

[9] Development of a several 10kW class circular-flat-type low-temperature operation SOFC system, Result report symposium 2007, New Energy and Industrial Technology Development Organization in Japan, http://www.nedo.go.jp/informations/events/200623/26_7.pdf, (in Japanese)

[10] Yasuda I., Development of Hydrogen Production Technology for Fuel Cell, Energy Synthesis Engineering, Vol. 28, No.2, (2005) (in Japanese)

[11] J. Mathiak, A. Heinzel, J. Roes, Th. Kalk, H. Kraus and H. Brandt, Coupling of a 2.5 kW steam reformer with a 1 kW PEM fuel cell, Journal of Power Sources, Vol. 131, No.1-2, (2004), 112-119.

[12] K. Oda, A Small-scale Reformer for Fuel Cell Application, Sanyo technical review, Vol. 31, No.2, (1999), 99-106. (in Japanese)

[13] Andrew L. Dicks, R. G. Fellows, C. Martin Mescal, Clive Seymour, A study of SOFC–PEM hybrid systems, Journal of Power Sources, Vol. 86, No. 1-2, (2000), 501-506.

[14] Mikkola, M., Experimental Studies on Polymer Electrolyte Membrane Fuel Cell Stacks, Master's thesis submitted in partial fulfillment of the requirements for the degree of Master of Science in Technology, Helsinki University of Technology, (2001), 58-79.

[15] Alan S. Feitelberg, Donald F. Rohr Jr, Operating line analysis of fuel processors for PEM fuel cell systems, International Journal of Hydrogen Energy, Vol. 30, No. 11, (2005), 1251-1257.

[16] K. Narita, "The Research on Unused Energy of the Cold Region City and Utilization for the District Heat and Cooling", Ph.D. thesis, (1996), Hokkaido University. (in Japanese)

Captions

Fig. 1 Microgrid model of a power system

Fig. 2 SOFC-PEFC combined power system

Fig. 3 Operation model of fuel cell systems A and B

Fig. 4 Power generation efficiency of the SOFC and PEFC, and reformer efficiency

Fig. 5 Power division rate of fuel cell systems A and B
(a) Operation pattern of the SOFC and PEFC
(b) Exhaust heat model of the SOFC
(c) Characteristics of reformed gas production
(d) Time shift operation of the reformed gas

Fig. 6 Energy demand pattern of the microgrid. 30 houses in Sapporo-city, Japan.
(a) Power demand model
(b) Heat demand model

Fig. 7 Power demand model of the microgrid
(a) Compressed load pattern
(b) Extended load pattern

Fig. 8 Power demand pattern of the microgrid (30 houses in Sapporo, Japan, a representative day in February)

Fig. 9a 23 kW SOFC system
Load factor and efficiency of the fuel cell
Fuel consumption of the boiler and fuel cell
Heat storage

Fig. 9b 23 kW PEFC system

Fig. 9c 17.6 kW SOFC and 6.8 kW PEFC combined system

Fig. 9 Analysis results of daily operation planning

Fig. 10 Analysis results of daily operation planning with the compressed load pattern (14.2 kW SOFC and 4.9 kW PEFC combined system)
Load factor and efficiency of the fuel cell

Fuel consumption of the boiler and fuel cell

Fig. 11 Analysis results of daily operation planning with the extended load pattern (21.8 kW SOFC and 7.4 kW PEFC combined system)

Fig. 12 Fuel consumption of each system under the average load pattern

Fig. 13 Load factor and efficiency of the fuel cell under the average load pattern

Fig. 14 Analysis results of the average power generation efficiency of each system

Fig. 15 Comparison of each system. The annual average result of the SOFC combined system when using 100% average load.

Fig. 16 Influence of the SOFC-PEFC combined system on the load characteristics. The annual average result of the SOFC-PEFC combined system when using 100% average load.

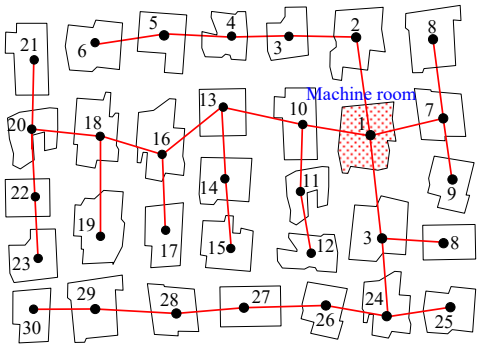

Fig. 1 Microgrid model of a power system

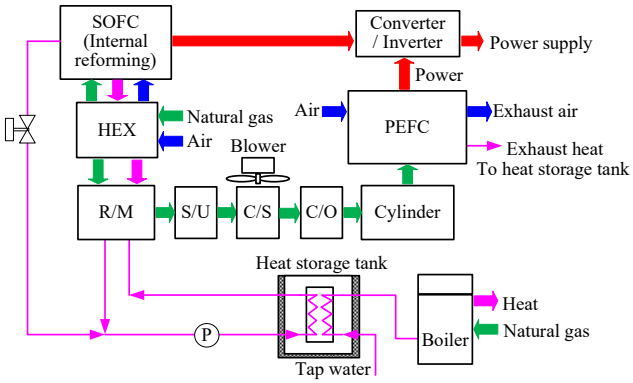

C/O : CO oxidation unit, C/S : Condenser unit, HEX : Heat exchanger, R/M : Reformer, S/U : Shift unit

Fig. 2 SOFC-PEFC combined power system

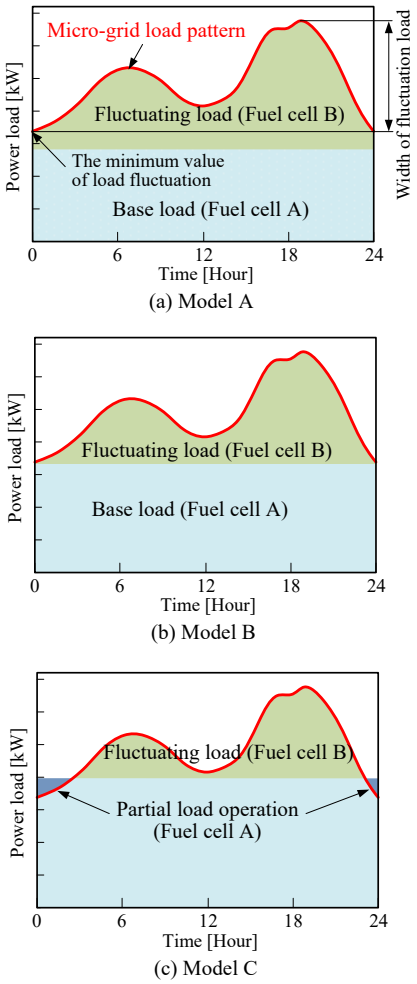

Fig. 3 Operation model of fuel cell systems A and B

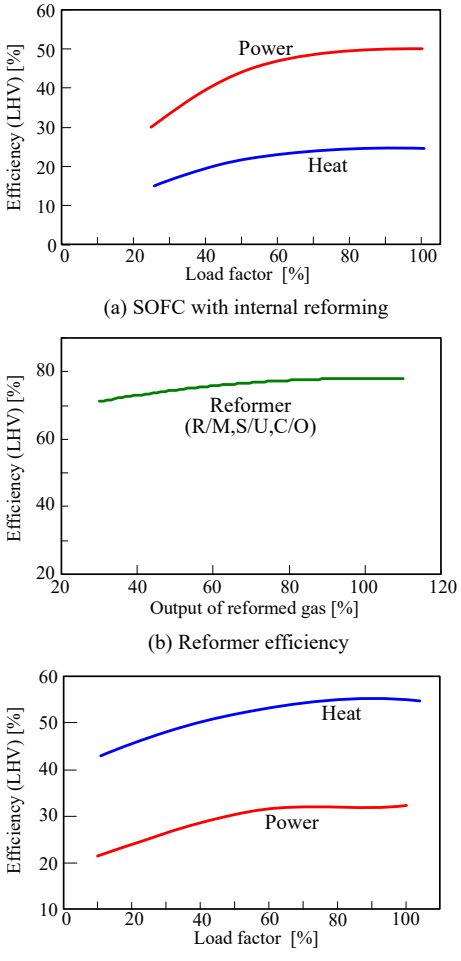

Fig. 4 Power generation efficiency of the SOFC and PEFC, and reformer efficiency

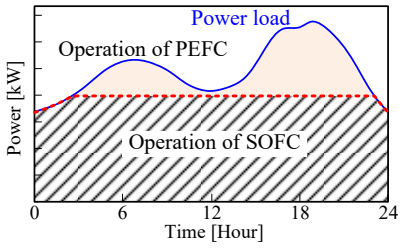

(a) Operation pattern of the SOFC and PEFC

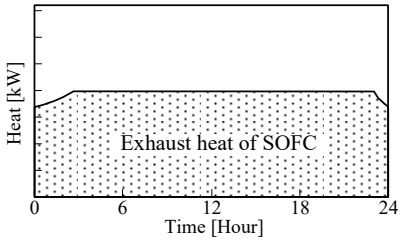

(b) Exhaust heat model of the SOFC

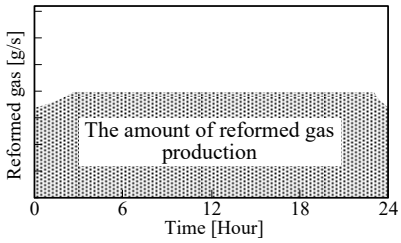

(c) Characteristics of reformed gas production

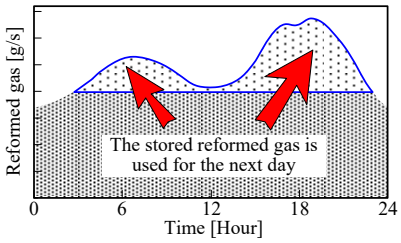

(d) Time shift operation of the reformed gas

Fig. 5 Power division rate of fuel cell systems A and B

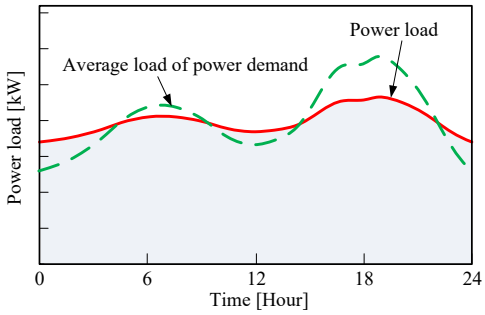

(a) Compressed load pattern

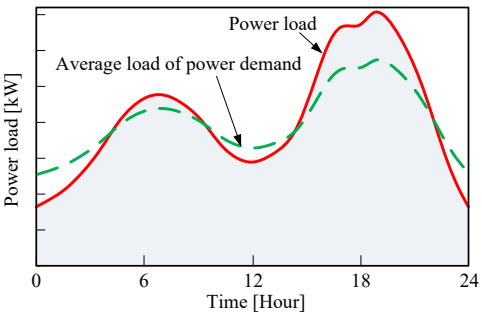

(b) Extended load pattern

Fig. 7 Power demand model of the microgrid

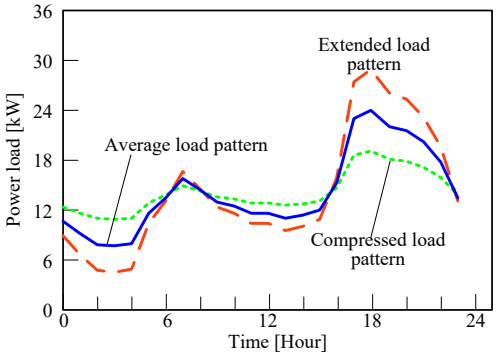

Fig. 8 Power demand pattern of the microgrid
(30 houses in Sapporo, Japan, representative day in February)

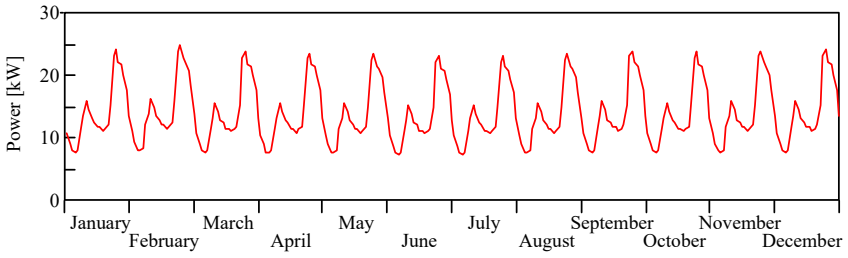

(a) Power demand model in representative day

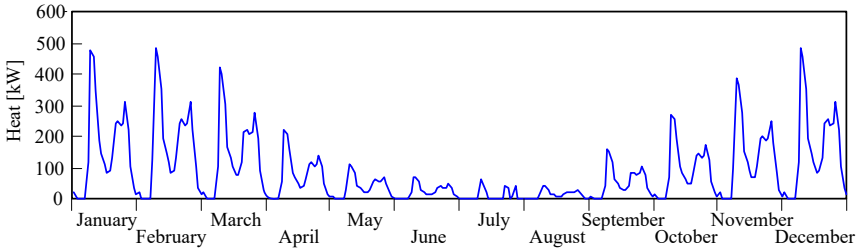

(b) Heat demand model in representative day

Fig. 6 Energy demand pattern of the microgrid. 30 houses in Sapporo-city, Japan.

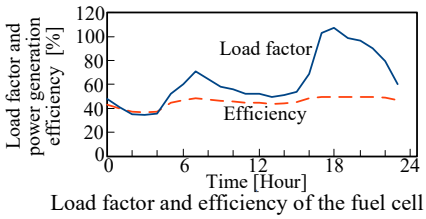

Load factor and efficiency of the fuel cell

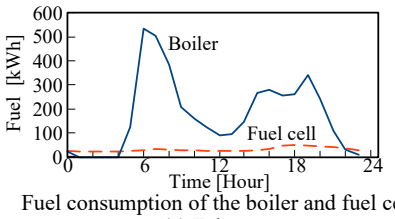

Fuel consumption of the boiler and fuel cell

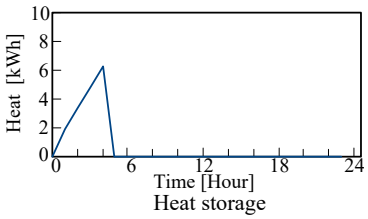

Heat storage

(a) February

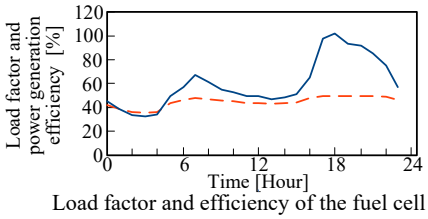

Load factor and efficiency of the fuel cell

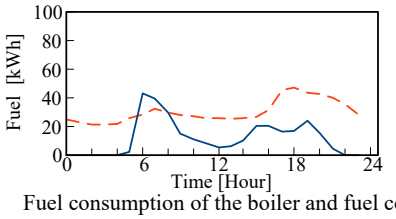

Fuel consumption of the boiler and fuel cell

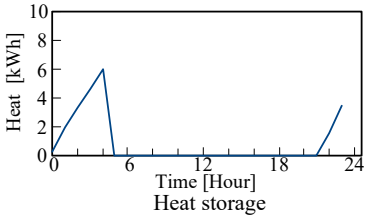

Heat storage

(b) August

Fig. 9a 23 kW SOFC system

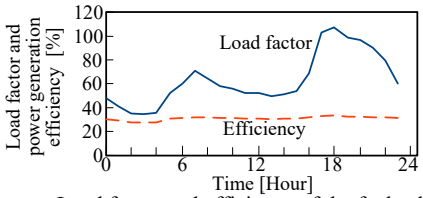

Load factor and efficiency of the fuel cell

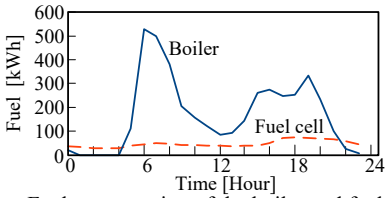

Fuel consumption of the boiler and fuel cell

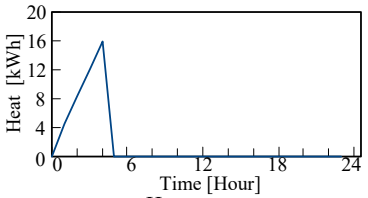

Heat storage

(a) February

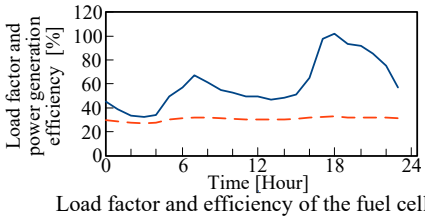

Load factor and efficiency of the fuel cell

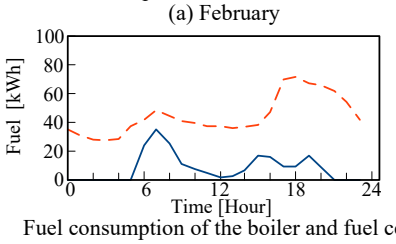

Fuel consumption of the boiler and fuel cell

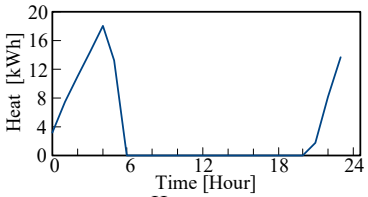

Heat storage

(b) August

Fig. 9b 23 kW PEFC system

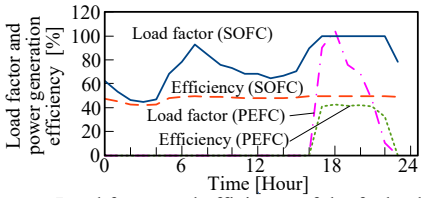

Load factor and efficiency of the fuel cell

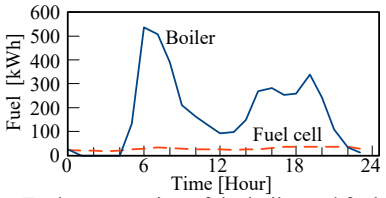

Fuel consumption of the boiler and fuel cell

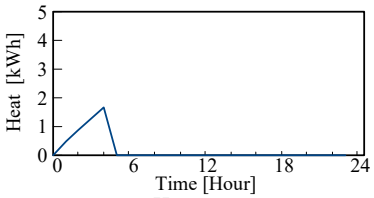

Heat storage

(a) February

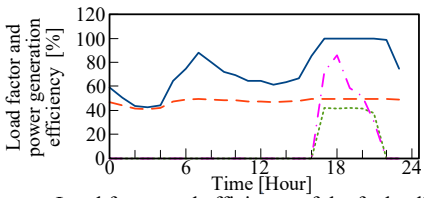

Load factor and efficiency of the fuel cell

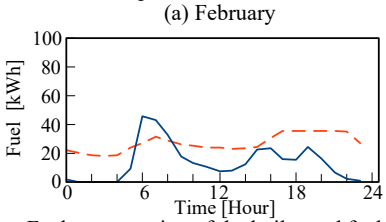

Fuel consumption of the boiler and fuel cell

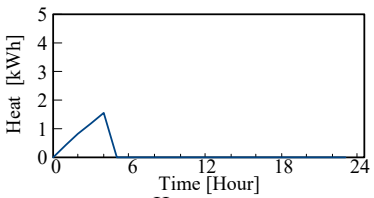

Heat storage

(b) August

Fig. 9c 17.6 kW SOFC and 6.8 kW PEFC combined system

Fig. 9 Analysis results of daily operation planning

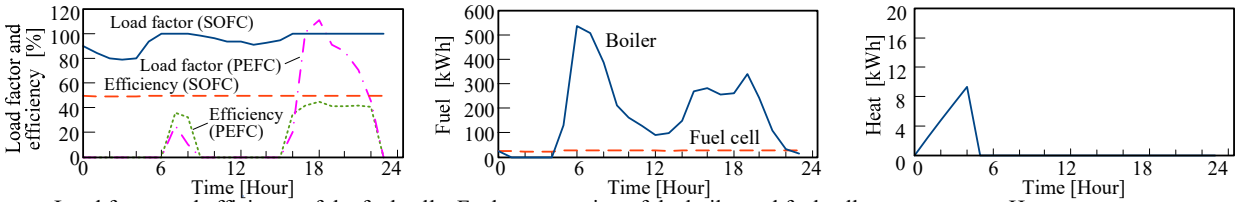

Load factor and efficiency of the fuel cell　Fuel consumption of the boiler and fuel cell　Heat storage

(a) February

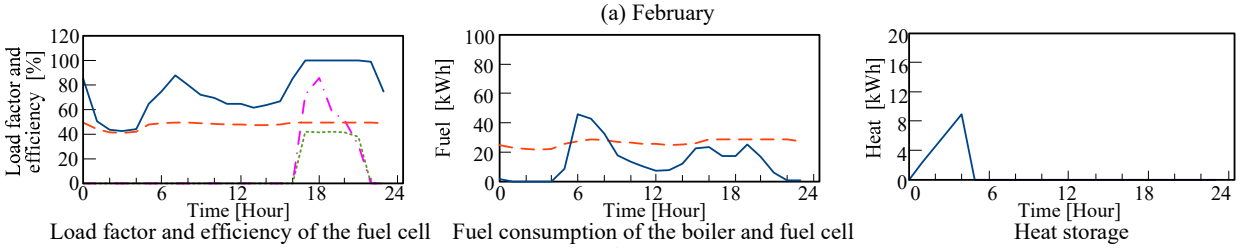

Load factor and efficiency of the fuel cell　Fuel consumption of the boiler and fuel cell　Heat storage

(b) August

Fig. 10 Analysis results of daily operation planning with the compressed load pattern
(14.2 kW SOFC and 4.9 kW PEFC combined system)

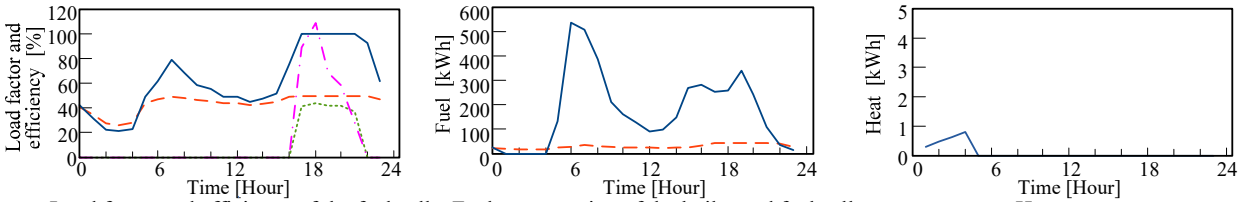

Load factor and efficiency of the fuel cell　Fuel consumption of the boiler and fuel cell　Heat storage

(a) February

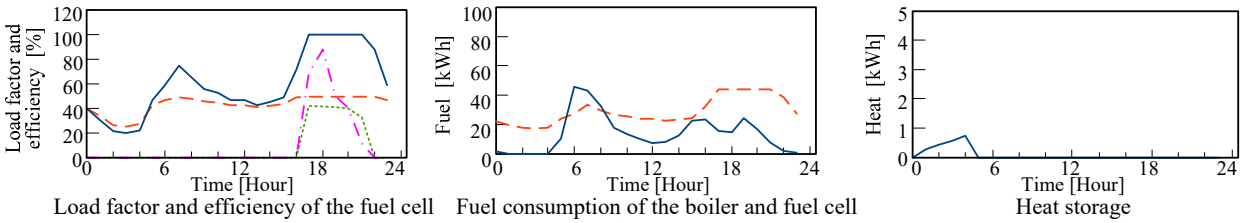

Load factor and efficiency of the fuel cell　Fuel consumption of the boiler and fuel cell　Heat storage

(b) August

Fig. 11 Analysis results of daily operation planning with the extended load pattern
(21.8 kW SOFC and 7.4 kW PEFC combined system)

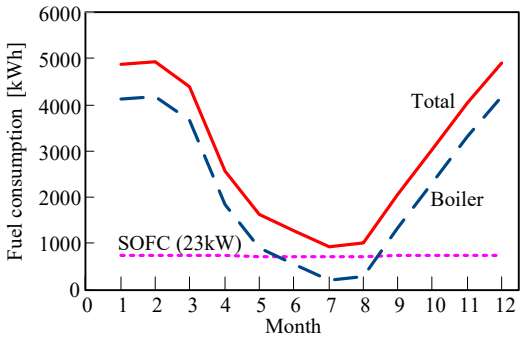

(a) SOFC system

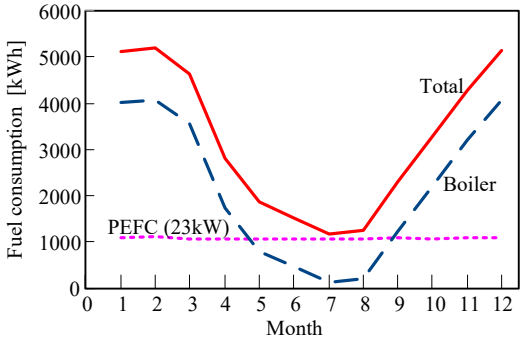

(b) PEFC system

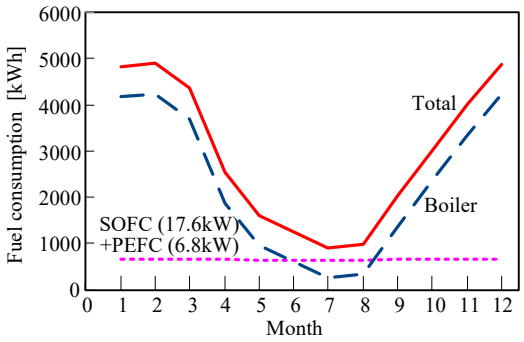

(c) SOFC-PEFC combined system

Fig. 12 Fuel consumption of each system under the average load pattern

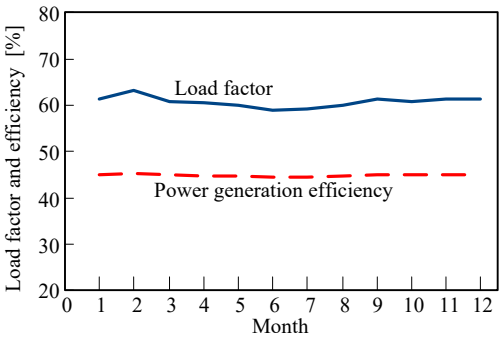

(a) SOFC (23kW) system

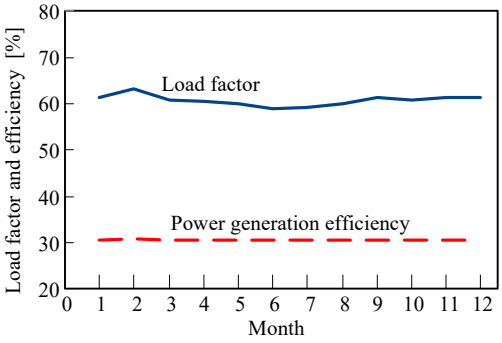

(b) PEFC (23kW) system

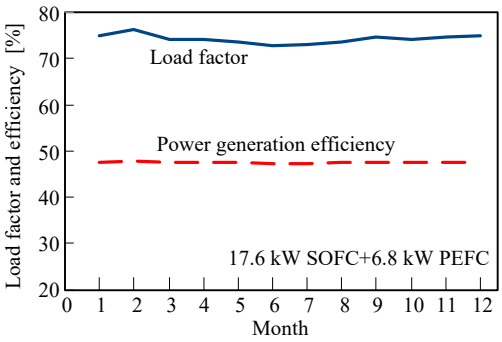

(c) SOFC (17.6kW) and PEFC (6.8kW) combined system

Fig. 13 Load factor and efficiency of the fuel cell under the average loadpattern

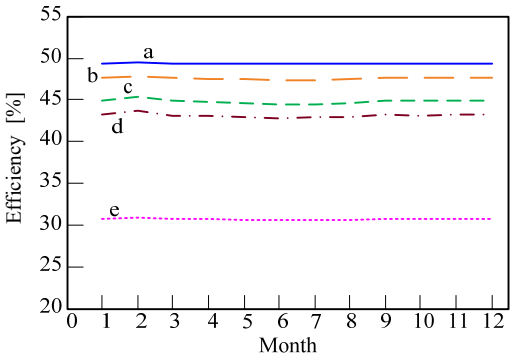

a : Compressed load pattern, 14.2 kW SOFC and 4.9 kW PEFC combined system
b : Average load pattern, 17.6 kW SOFC and 6.8 kW PEFC combined system
c : Average load pattern, 23 kW SOFC
d : Extended load pattern, 21.8 kW SOFC and 7.4kW PEFC combined system
e : Average load pattern, 23 kW PEFC

Fig. 14 Analysis results of the average power generation efficiency of each system

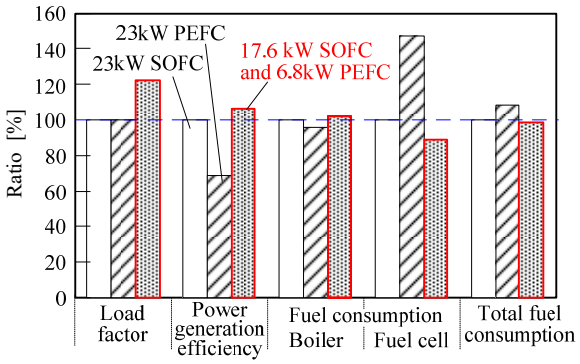

Fig. 15 Comparison of each system. The annual average result of the SOFC combined system when using 100% average load.

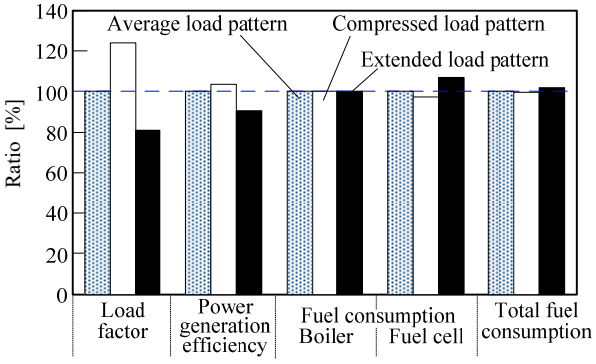

Fig. 16 Influence of the SOFC-PEFC combined system on the load characteristics. The annual average result of the SOFC-PEFC combined system when using 100% average load.